

Observation of Periodic Orbits on Curved Two-dimensional Geometries

M. Avlund¹, C. Ellegaard¹, M. Oxborrow², T. Guhr³, and N. Søndergaard⁴

¹*Niels Bohr Institutet, Blegdamsvej 17, 2100 København Ø, Denmark*

²*National Physical Laboratory, Hampton Road, Teddington, TW11 0LW, UK*

³*Fakultät für Physik, Universität Duisburg–Essen, Lotharstraße 1 47057 Duisburg, Germany*

⁴*Matematisk Fysik, LTH, Lunds Universitet, Box 118, 22100 Lund, Sweden*

(Dated: May 15, 2021)

We measure elastomechanical spectra for a family of thin shells. We show that these spectra can be described by a “semiclassical” trace formula comprising periodic orbits on geodesics, with the periods of these orbits consistent with those extracted from experiment. The influence of periodic orbits on spectra in the case of two-dimensional curved geometries is thereby demonstrated, where the parameter corresponding to Planck’s constant in quantum systems involves the wave number and the curvature radius. We use these findings to explain the marked clustering of levels when the shell is hemispherical.

PACS numbers: 05.45.Mt, 43.40.Ey, 62.20.D-

When studying spectra of quantum systems, semiclassical, in particular periodic orbit theory, provides a powerful connection to the dynamics of the analogous classical system [1–4]. Considerable progress was recently made in understanding generic statistical properties of quantum chaotic systems [5]. Furthermore, spectra of specific systems can be constructed from periodic orbits, prominent examples are the Hydrogen atom in a strong magnetic field [6], the Helium atom [7] as well as regular and chaotic two-dimensional billiards [2, 3]. Microwave experiments in flat cavities [8] are most useful because, in two dimensions, the Helmholtz equation for the electrical field formally coincides with the Schrödinger equation.

Do the concepts of quantum chaos carry over to other wave phenomena? — Elasticity, i.e. mechanical vibrations, is a particularly interesting testing ground. The governing equations and the boundary conditions are different from the ones in quantum mechanics. Moreover, different modes (pressure and shear) are present and propagate with different velocities, in case of anisotropy even depending on the directions. Hence, a transfer of quantum chaos ideas to elastic systems is a worthwhile endeavor in its own right. The bulk waves in three-dimensional aluminum blocks have the same statistical features as known for quantum chaotic systems [9]. Remarkably, even much more subtle features have been measured and understood in a framework transferred from quantum chaos: parametric statistics [10], transport and localization properties in three-dimensional blocks [11], the statistics of elastic displacements, i.e. “wave functions”, in two-dimensional plates [12] and Wannier–Stark ladders in quasi-one-dimensional elastic systems [13].

In this contribution, we measure spectra of thin elastic shells and explain certain characteristics by periodic orbits. This is, to the best of our knowledge, the first experimental identification of periodic orbit features on curved shells. We have two goals. First, we show that periodic

orbit theory can be applied to the shells. This is non-trivial because of the curvature and because the modes are a combination of flexural and in-plane fields. They are in general described by a system of partial differential equations of high order [14], very different from the Schrödinger equation which is the starting point in quantum chaos. Second, we will use this insight to explain a striking clustering effect in the spectra. These findings are not only of conceptual but also of practical importance. Metallic shells are ubiquitous in technology and every day life, ranging from auto bodies to micro-electro-mechanical systems. Since the calculation of spectral features from the wave equation is often tremendously complicated, an understanding in terms of simpler geometric quantities, the periodic orbits, might be of considerable interest.

The shells we employ are objects of revolution as shown in Fig. 1. They form a family of constant mid-surface area parameterized by the opening angle θ_0 measured

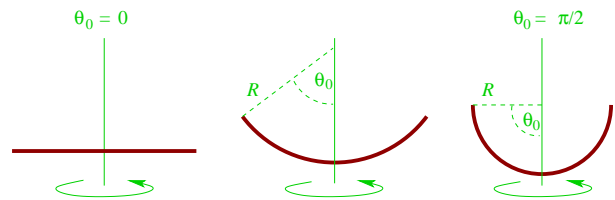


FIG. 1: (Color online) Shells of revolution with opening angle θ_0 and curvature radius R .

from the axis of revolution, whereas R is the θ_0 dependent curvature. For $\theta_0 = \pi/2$, we have a hemisphere, the angle $\theta_0 = 0$ formally corresponds to the planar disk. Figure 2 displays the aluminum shells used in the experiment, the opening angles are $\theta_0 = 0^\circ, 25^\circ, 52^\circ$ and 90° . Each shell is 2 mm thick although for the hemisphere three thicknesses were studied. The disk has a diameter of 80 mm, the other shells were made in such a way that



FIG. 2: (Color online) Aluminum shells used in the experiment. From left to right, the opening angle is $\theta_0 = 0^\circ, 25^\circ, 52^\circ$ and 90° .

all mid-surface areas are equal. The shells were carved from a solid aluminum block to avoid any internal strain which inevitably occurs when producing curved objects by bending a plate. It was carefully made sure that the cut defining the boundary was along the radius, as seen in Fig. 1. This is important to prevent coupling between flexural and membrane-like modes.

We used the experimental setup developed in our previous studies [10, 12]. It has a very high resolution, the quality factor $Q = f/\Delta f$ is typically about 10^5 where f and Δf are position and width in frequency of a given resonance, respectively. We accumulated data in the frequency range $0 \text{ kHz} \leq f \leq 800 \text{ kHz}$. In the measurement, the shells are only supported by three 1 mm ruby spheres which minimize the elastic coupling to the rest of the setup. The acoustic coupling to the air is significantly reduced by putting the setup into a vacuum chamber whose inside is held at 10^{-3} Torr. Flexural (bending) modes and membrane-like (stretching and shearing) modes are excited. The resulting spectra are displayed in Fig. 3. A visual inspection immediately reveals that the spectra

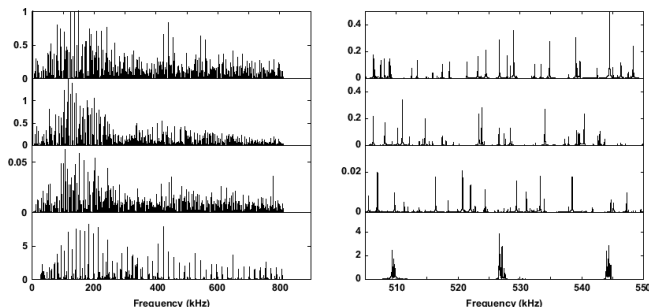


FIG. 3: (Color online) Measured spectra for the shells with opening angles $\theta_0 = 0^\circ, 25^\circ, 52^\circ$ and 90° from top to bottom.

for the disk and the shells with opening angle $\theta_0 < \pi/2$ look rather similar. For the hemisphere with $\theta_0 = \pi/2$,

however, the levels are structured in clusters which are almost equally spaced. The clustering was already found in Ref. [15] by numerically solving the equations for thin shells [14]. In the following, we will use periodic orbits to give a clear and intuitive explanation of this striking effect.

Our reasoning will be in the spirit of semiclassical analysis for quantum systems. We demonstrate that the in-plane excitations can be described by a sum over periodic orbits, i.e. by a trace formula akin to the ones in quantum chaos [1–4]. This goes well beyond previous work on the celebrated whispering gallery modes [2], on the ray-description of seismic waves [16] as well as on the identification of periodic orbits in elastic spectra of three dimensional systems [10, 17]. Trace formulae are

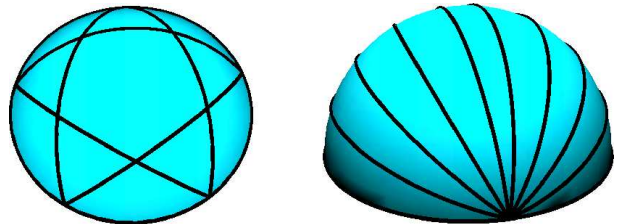


FIG. 4: (Color online) Geodesic pentagram and diameters on the spherical cap.

different for regular and chaotic systems. If the wave equation describing shell vibrations were scalar, all our shells would be integrable. The complexity of the wave equation for thin shells [14] modifies that picture. The wave equation can be separated into an angular part depending on the angle of revolution and a “radial” part depending on the angle θ measured from the axis of revolution with $0 \leq \theta \leq \theta_0$. In the “semiclassical” approximation [18] the waves are approximated by the motion of a fictitious particle. The main insight is that this motion takes place on the geodesics of the shells as in Fig. 4. The rôle of Planck’s constant compared to a typical action is here played by $1/kR$, where k is the wave number. To leading order, the flexural and the membrane-like motion decouple, i.e. yield two separate equations of motion for the fictitious particle. Hence, the flexural motion is integrable. There are two degrees of freedom on the shells and two constants of motion, the energy and the angular momentum with respect to the axis of revolution. The membrane-like motion, however, has two polarizations, one longitudinal (L, pressure) and one transverse (T, shear) mode. They are always coupled upon reflections at the boundary. In this sense, the membrane-like motion is not integrable.

The measured spectrum in Fig. 3 lowest plot shows evidence of eigenvalue clusters which are separated by a slowly increasing spacing in frequency. The first clusters appear only after a gap. At medium to high fre-

quencies the spacing appears constant and for thin hemispheres agrees well with the spacing coming from purely T-polarized orbits. Furthermore, the extracted discrete

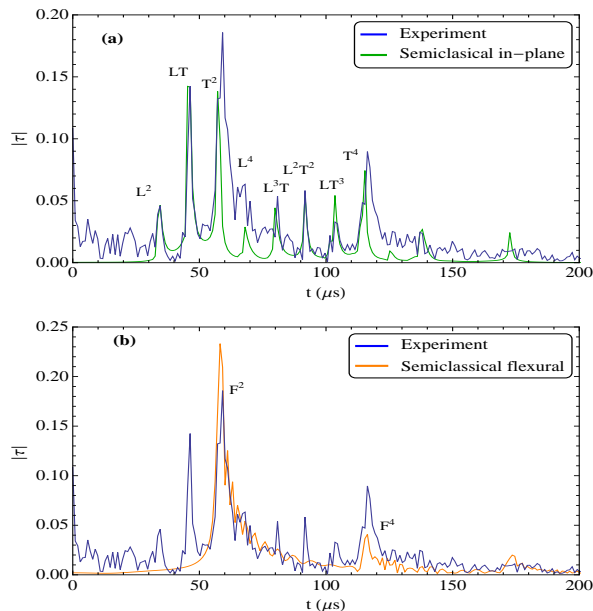


FIG. 5: (Color online) Time spectrum of spectral fluctuations containing **L**ongitudinal, **T**ransverse (a) and **F**lexural segments of orbits (b).

spectrum show fluctuations well described by certain time periods, see Fig. 5, corresponding to fixed spacings in frequency which we attribute to periodic orbits in the following. From shell theory, we therefore focus on the in-plane deformation field for which dispersion is linear and results in orbit actions linear in frequency. We shall also touch briefly on the flexural mode as its dispersion approaches linear at the higher frequencies probed in our experiment.

The in-plane theory results from ignoring the flexural motion in the Kirchoff-Love shell theory [14, 15] and leads to

$$\frac{E}{2} [(1 + \nu) \Delta \mathbf{u} + (1 - \nu) \nabla \nabla \cdot \mathbf{u}] + \rho \omega^2 \mathbf{u} = 0 \quad (1)$$

when dropping curvature terms in the ray limit. The constants E and ν are the elastic modulus of extension and the ratio of Poisson corresponding to the plane stress approximation used in plates [14]. Up to further curvature terms, this curved version of Navier-Cauchy's elastic equation is rewritten by re-expressing the covariant vector laplacean $\nabla_a \nabla^a$ in terms of two-dimensional curls and a gradient on a divergence [19]. Consequently, the elastic field can be decomposed in a gradient field and a curl field corresponding to longitudinal and transverse polarization each satisfying a curved scalar Helmholtz equation:

$$(\Delta + z_j^2) u^{(j)} = 0 \quad (2)$$

with $j = L, T$ a polarization index in the following and $z_j = k_j R$ dimensionless wave numbers obeying $z_T = \kappa z_L$ with $\kappa = c_L/c_T$ the ratio of propagation speeds in plates. On the sphere, deformations are therefore expanded using Legendre functions $\{P, Q\}_n^m(\cos \theta) \exp(im\phi)$ with $n = l_j$ a polarization dependent angular momentum obeying $z_j^2 = l_j(l_j + 1)$. We impose free boundary conditions: the integrated stress tensor across the thickness of the shell vanishes at a boundary. Thus, the normal components of the stress resultant vanishes: $N_{\hat{\theta}a} = 0$ at $\theta = \pi/2$ with $a = \hat{\theta}, \hat{\phi}$ [14]. The spectrum is then found by a two-by-two determinantal condition.

As in the scalar problem [18] we use the method of scattering quantization [20] and consider the dynamics of a ray of polarization j in the angular momentum variable l_j evolving under the condition that L_z is constant. By elementary calculations we find this conservation law to be equivalent to the laws of reflection and refraction for the ray. For the derivation of a trace formula we therefore sum over $m \equiv L_z = l_L \sin \theta$ with θ the incidence angle with respect to the normal. Except for the increase in complexity, we find a very similar result as in [18]: there is a scattering matrix composed of a propagation part and a reflection/refraction part.

The propagation part over a single great arc of the hemisphere is found to be $\exp(-i\pi l_j)$ with $l_j \approx z_j + 1/2$ with the $1/2$ related to the caustic phase shift. The free propagation over the sphere is then independent of m and no saddle point integration is needed as in the case of an opening angle different from $\pi/2$.

The total m -dependence resides only in the reflection coefficients α_q used for constructing an orbit q . For large l each reflection coefficient is asymptotic to the classical reflection coefficient and a slowly varying function of m , so the sum over m is well approximated by an integral and yields

$$\begin{aligned} \text{tr } \alpha_q &\approx \int_{-l_L}^{l_L} dm \alpha_q \left(\frac{m}{l_L} \right) \\ &= l_L \int_{-\pi/2}^{\pi/2} d\theta \cos \theta \alpha_q(\theta) \equiv l_L \overline{\mathcal{A}}_q. \end{aligned} \quad (3)$$

The final result of our calculations is that the oscillating number of states $d\tilde{N}$ in a frequency interval df coming from orbits is given to leading order as

$$d\tilde{N} = \tilde{\rho}_{IP}(f) df \approx l_L \sum_{p^r} \overline{\mathcal{A}}_{p^r} \cos(\pi r l_p) dl_p, \quad (4)$$

where p^r is a closed orbit containing an r 'th repeat of a prime ray sequence p and $l_p = n_L l_L + n_T l_T$ with n_L, n_T integers. We find it useful to group orbits with identical actions such as $(LT)^2$ and $LLTT$ and denote the family L^2T^2 . In practice $\overline{\mathcal{A}}$ for each family is calculated numerically. Notably, fluctuations grow linearly with frequency to leading order. Rayleigh edge orbits are omitted as their contribution is of order f^0 only.

For completeness we include transverse rays with incidence angles beyond the critical angle for conversion for which the reflection coefficient is of unit modulus. Consequently, this part of phase space for T-polarized orbits leads to clusters of closely grouped states [21]. Ref. [21] states that (4) should hold in general; here for the first time we present an explicit study in a ray splitting case. We give a parallel treatment to the flexural orbits using their corresponding reflection coefficients [22] and dispersion relation [23]. Here we settle for one extracted from the numerical solution of a whole spherical shell due to its larger spectral range.

The simulated spectral fluctuations of the hemisphere used in our experiment have a period spectrum depicted in Fig. 5: the (a) spectrum shows clear evidence of in-plane orbits. The inclusion of the flexural modes in (b) gives trains of peaks with the main peaks close to those of the transverse. This is because at higher frequencies the flexural dispersion approaches the linear with the flexural speed approaching the Rayleigh speed which is just below the transverse speed. Furthermore, the clusters in the transducer signal we checked to agree well with the peaks in the flexural fluctuations.

Why is the spectrum for the hemisphere so different? This is illustrated in Fig. 4. For all opening angles, all periodic orbits are geodesic polygons, Fig. 4 (left) shows the pentagram as an example. As the opening angle increases, the surface enclosed by the polygons becomes larger. At $\theta_0 = 90^\circ$, this surface is the entire hemisphere. Hence all polygons degenerate to the orbit on the base of the hemisphere. The diameter orbit shown in Fig. 4 (right) is the exception: there is only one such orbit for $\theta_0 < 90^\circ$, because it must go through the north pole. At $\theta_0 = 90^\circ$, however, all geodesic lines connecting opposite points on the base are diameter orbits. These drastic changes in the periodic orbit structure reflect the equally drastic changes in the spectrum when the opening angle reaches 90° . Formula (4) gives the precise mathematical connection.

In conclusion, we measured high-resolution spectra of a family of open spherical shells and saw clear evidence of in-plane behavior. For this we developed a trace formula for the density of states which agree well with experiment. The amplitudes of the fluctuations were not entirely as in experiment, still the location of the periods of the experimental fluctuations agreed well with theory. Hence, we have presented a first identification of periodic orbit structures on curved geometries. From the simple form of the trace formula we expect it to be easy to generalize and apply to other wave equations on the hemisphere. Thus, when applied to the flexural mode, also the clusters of the transducer signal are described.

We thank Sir M. Berry and E. Bogomolny who already a long time ago suggested shells to us as an important

object of study. TG acknowledges support from Deutsche Forschungsgemeinschaft (SFB/TR12, “Symmetries and Universality in Mesoscopic Systems”), NS is grateful for support from Det Svenska Vetenskapsrådet.

-
- [1] M.C. Gutzwiller, *Chaos in Classical and Quantum Mechanics*, Springer, New York (1990)
 - [2] M. Brack and R.K. Bhaduri, *Semiclassical Physics*, Frontiers in Physics, Vol. **96**, Addison-Wesley, Reading (1997)
 - [3] H.J. Stöckmann, *Quantum Chaos — An Introduction*, Cambridge University Press, Cambridge (1999)
 - [4] F. Haake, *Quantum Signatures of Chaos*, 2nd ed., Springer, Heidelberg (2001)
 - [5] S. Heusler, S. Müller, A. Altland, P. Braun, and F. Haake, Phys. Rev. Lett. **98**, 044103 (2007)
 - [6] H. Friedrich and D. Wintgen, Phys. Rep. **183**, 37 (1989)
 - [7] D. Wintgen, K. Richter, and G. Tanner, Chaos **2**, 19 (1992)
 - [8] H.J. Stöckmann and J. Stein, Phys. Rev. Lett. **64**, 2215 (1990); H.D. Gräf, H.L. Harney, H. Lengeler, C.H. Lewenkopf, C. Rangacharyulu, A. Richter, P. Schardt, and H.A. Weidenmüller, Phys. Rev. Lett. **69**, 1296 (1992)
 - [9] R.L. Weaver, J. Acoust. Soc. Am. **85**, 1005 (1989); C. Ellegaard, T. Guhr, K. Lindemann, H.Q. Lorensen, J. Nygård, and M. Oxborrow, Phys. Rev. Lett. **75**, 1546 (1995)
 - [10] P. Bertelsen, C. Ellegaard, T. Guhr, M. Oxborrow, and K. Schaadt, Phys. Rev. Lett. **83**, 2171 (1999)
 - [11] R.L. Weaver and O. Lobkis, J. Sound Vib. **231**, 1111 (2000)
 - [12] K. Schaadt, T. Guhr, C. Ellegaard, and M. Oxborrow, Phys. Rev. **E68**, 036205 (2003)
 - [13] L. Gutiérrez, A. Diaz-de-Anda, J. Flores, R.A. Méndez-Sánchez, G. Monsivais, and A. Morales, Phys. Rev. Lett. **97**, 114301 (2006)
 - [14] H. Kraus, *Thin Elastic Shells*, Wiley, New York (1967)
 - [15] F.I. Niordson, Int. J. Solids Structures **24**, 947 (1988)
 - [16] F.A. Dahlen and J. Tromp, *Theoretical Global Seismology*, Princeton University Press, Princeton (1998)
 - [17] D. Delande, D. Sornette, and R.L. Weaver, J. Acoust. Soc. Am. **96**, 1873 (1994)
 - [18] N. Søndergaard and T. Guhr, J. Phys. **A41**, 075309 (2008)
 - [19] N. Berline, E. Getzler, and M. Vergne *Heat Kernels and Dirac Operators*, Springer, New York (2004)
 - [20] U. Smilansky in *Les-Houches Summer School on mesoscopic quantum physics*, edited by E. Akkermans et al., North-Holland (1994)
 - [21] Y. Safarov and D. Vassiliev in *Spectral Theory of Operators*, edited by S.Gindikin, AMS Translations, ser.2, **150** (1992)
 - [22] E. Bogomolny and E. Hugues Phys. Rev. **E57** 5404 (1998)
 - [23] A.D. Pierce, Structural Acoustics, ASME, NCA Vol. 12, AMD Vol. 128, 195 (1991); A.D. Norris and D.A. Rebinsky, J. Vib. Acoust. **116**, 457 (1994)